Inorg. Chem. **2003**, *42*, 3856–3864

Conformational Preferences Driven by the *C*-Methyl Substituent in Chelated *o*-Diphenylphosphino-α-methyl-*N,N*-dimethylbenzylamine Rhodium Complexes

M. Aránzazu Alonso, Juan A. Casares, Pablo Espinet,* and Katerina Soulantica

Química Inorgánica, Facultad de Ciencias, Universidad de Valladolid, E-47005 Valladolid, Spain

A. Guy Orpen and Hirihattaya Phetmung

School of Chemistry, University of Bristol, Bristol BS8 1TS, U.K.

Received February 3, 2003

The stereochemistry of the chelate rings of a number of rhodium aminophosphine complexes is studied by NMR spectroscopy. The similarity in the variable-temperature behavior for the different compounds is consistent with them having in common highly preferred chelate ring conformations. The six-membered metallacycle of coordinated (*R*)-P*N (P*N = *o*-diphenylphosphino-α-methyl-*N,N*-dimethylbenzylamine) adopts a δ conformation in the solid state. NMR experiments indicate that this conformation is strongly favored in solution as well. The preferred sense of helicity is imposed by the absolute configuration of the stereogenic carbon atom on the ligand, which exerts an important steric control. The complex $[Rh(TFB)\{(C_6H_4CHMeNMe_2)_2P(C_6H_4CHMeNHMe_2)\}](BF_4)_2 \cdot H_2O \cdot Me_2CO$ crystallizes in the monoclinic space group P2(1) with $a = 12.0548(11)$ Å, $b = 16.139(2)$ Å, $c = 12.1804(10)$ Å, $\beta = 100.742(9)°$, $Z = 4$.

Introduction

Chiral multidentate ligands combining phosphorus and nitrogen donor atoms are of interest for enantioselective homogeneous catalysis due to their efficiency in reactions such as allylic alkylation, allylic amination, hydroboration, hydrosilylation, or Grignard cross-coupling.[1]

The steric effect of the ligands is a crucial factor for effective chirality induction in stereoselective reactions at the metal center. An essential component of asymmetric induction for many enantioselective catalytic systems is the conformation of the chiral ligand framework. Conformational rigidity is a frequent feature of highly enantioselective catalysts.[1b]

The conformational behavior of chelates with more than five atoms in the ring is open to the coexistence of several conformers of similar energy.[2,3] The introduction of substituents in the ring modifies their energy and can eventually lead to conformational locking by favoring one particular conformer with respect to the others, or by slowing the interchange between them.

NMR spectroscopy is the technique of choice for studying conformation interconversions in solution. The methodology for the analysis of asymmetric induction is well established and has been applied to different P,N-donor ligands used in catalysis.[4]

We are interested in the structural properties of the P,N-multidentate ligands and have reported on the coordination

* Author to whom correspondence should be addressed. E-mail: espinet@qi.uva.es.

(1) (a) Sawamura, M.; Ito, Y. *Chem. Rev.* **1992**, *92*, 857. (b) Ojima, I. *Catalytic Asymmetric Synthesis*; VCH: New York, 1993. (c) Salvakumer, K.; Valentini, M.; Pregosin, P. S. *Organometallics* **2000**, *19*, 1299. (d) Brunner, H.; Deml, I.; Dirnberger, W.; Ittner, k. P.; Reisser, W.; Zimmernam, M. *Eur. J. Inorg. Chem.* **1999**, 51. (e) Blöchl, P. E.; Togni, A. *Organometallics* **1996**, *15*, 4125. (f) Abbenhuis, H. C. L.; Burckhardt, U.; Gramlich, V.; Martelletti, A.; Spencer, J.; Steiner, I.; Togni, A. *Organometallics* **1996**, *15*, 1614. (g) Togni, A. *Angew. Chem., Int. Ed. Engl.* **1996**, *35*, 1475.

(2) Harrowfield, J. M.; Wild, S. B. In *Comprehensive Coordination Chemistry*; Wilkinson, S. G., Gillard, R. D., McCleverty, J. A., Eds.; Pergamon Press: Oxford, 1987; Vol. 1, Chapter 5, p 179.

(3) (a) Clifford, J. H.; Palmer, J. A. *Coord. Chem. Rev.* **1982**, *44*, 1. (b) Brubaker, G. R.; Johnson, D. W. *Coord. Chem. Rev.* **1984**, *53*, 1.

(4) (a) Berger, H.; Nesper, R.; Pregosin, P. S.; Rüegger, H.; Wörle, M. *Inorg. Chim. Acta* **1994**, *76*, 1520. (b) Pregosin, P. S.; Salzmann, R.; Togni, A. *Organometallics* **1995**, *14*, 842. (c) Carmona, D.; Lahoz, F. J.; Oro, L. A.; Lamata, M. P.; Viguri, F.; San José, E. *Organometallics* **1996**, *15*, 2961 (d). Albinati, A.; Eckert, J.; Pregosin, P. S.; Ruegger, H.; Salzmann, R.; Stoessel, C. *Organometallics* **1997**, *16*, 579. (e). Feiken, N.; Pregosin, P.; Trabesinger, G. *Organometallics* **1998**, *17*, 4510. (f) Crociani, B.; Antonaroli, S.; Di Vona, M. L.; Licoccia, S. *J. Organomet. Chem.* **2001**, *631*, 117. (g) Manzano, B. R.; Jalón, F. A.; Gómez-de la Torre, F.; López-Agenjo, A. M.; Rodríguez, A. M.; Mereiter, K.; Weissensteiner, W.; Sturm, T. *Organometallics* **2002**, *21*, 789−802.

10.1021/ic034117a CCC: $25.00
Published on Web 05/15/2003

Scheme 1

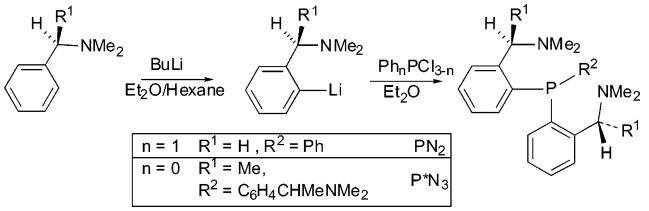

Scheme 2

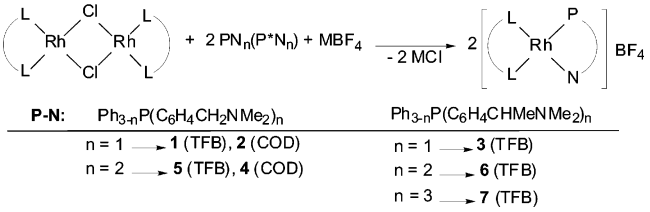

P-N:	$Ph_{3-n}P(C_6H_4CH_2NMe_2)_n$	$Ph_{3-n}P(C_6H_4CHMeNMe_2)_n$
	n = 1 → **1** (TFB), **2** (COD)	n = 1 → **3** (TFB)
	n = 2 → **5** (TFB), **4** (COD)	n = 2 → **6** (TFB)
		n = 3 → **7** (TFB)

and fluxional behavior of $P(CH_2CH_2Py)_nPh_{3-n}$ (Py = 2-pyridyl) Pd and Rh complexes and complexes with other pyridylphosphine ligands.[5] In this paper, we explore two families of other P,N-multidentate ligands, namely, $P(C_6H_4CH_2NMe_2)_nPh_{3-n}$ (PN_n) and the enantiomerically pure $P(C_6H_4CHMeNMe_2)_nPh_{3-n}$ (P^*N_n). In principle, any nonplanar P,N-chelate ring can adopt a chiral conformation and thereby endow chirality on the complex as a whole. Apart from a chiral conformation, some of these ligands contain stereogenic centers, either at phosphorus or at the α-carbon atom of the ligand framework. This work is focused on the study of analogies and differences between PN_n and P^*N_n complexes. The relationship between substituents, conformational preferences, and dynamic behavior is discussed, and the activation barriers for the different dynamic processes (exchange of amino groups, conformational inversion, olefin rotation) are analyzed.

Results

Synthesis of the Ligands. The new ligands $P(C_6H_4CH_2NMe_2)_2Ph$ (PN_2) and $P(C_6H_4CHMeNMe_2)_3$ (P^*N_3) were prepared according to Scheme 1, following the general procedure developed by Roundhill et al.[6]

Solution Structures and NMR Spectroscopy for the Diene Complexes. The Rh(diolefin) complexes were prepared from the corresponding $[(\mu\text{-}Cl)_2Rh_2(L\text{-}L)_2]$ species (L-L = TFB (tetrafluorobenzobicyclo[2.2.2.]octatriene, tetrafluorobenzobarralene) or COD (1,5-cyclooctadiene)) using the aminophosphines $P(C_6H_4CH_2NMe_2)_nPh_{3-n}$ (PN_n) and $P(C_6H_4CHMeNMe_2)_nPh_{3-n}$ (P^*N_n), as shown in Scheme 2. All of the compounds were characterized by elemental analysis, IR, and NMR (^1H, ^{31}P). Standard COSY $^1H-^1H$ and NOESY $^1H-^1H$ experiments were used to help with the assignments.

Chart 1

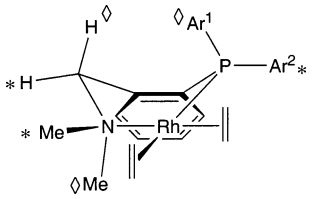

In all of the new complexes **1**−**7** the shift of the NMe_2 signals and ^{31}P resonances with respect to the free ligands support a bidentate P,N-chelate coordination.[7] The values of $^1J(Rh-P)$ are typical for square planar species of Rh(I).[8] As already reported by Roundhill et al. and by van Koten et al., the chelate ring puckering of the two *N*-methyl groups in this type of complex makes the benzylic protons and the PAr_2 groups diastereotopic (Chart 1).[6,9] In this low symmetry all of the diolefin protons are nonequivalent, and the ^1H spectrum at low temperature displays 12 signals for the COD protons and six signals for the TFB protons. In solution, the cationic products are fluxional. Their behavior in solution was studied by ^1H NMR at different temperatures and also by 2D phase sensitive ^1H NMR NOESY experiments.

Characterization and Dynamic Behavior of the New Derivatives (1−7). (a) Rhodium−PN_1−Diolefin and Rhodium−P^*N_1−Diolefin Complexes. The signals in the ^1H NMR spectrum of the complexes with PN_n ligand (**1** and **2**), including the olefinic hydrogens (trans to N or trans to P), have been fully assigned. The olefinic protons that usually are assigned by their chemical shifts[10] have been unambiguously assigned by the NOE effect observed between *N*-Me signals and the olefinic signals at lowest field (4.5−6.5 ppm depending on the complex, see Experimental Section).

The VT-^1H NMR analysis of $[Rh(TFB)(PN_1)]BF_4$ (**1**) and $[Rh(COD)(PN_1)]BF_4$ (**2**) shows the coalescence of the nonequivalent methyl group signals. The $\Delta G^{\ddagger}$ value has been calculated at the coalescence temperature (**1**, $\Delta G^{\ddagger} = 41.52 \pm 0.2$ kJ mol^{-1}, $T_c = 210.6$ K; and **2**, $\Delta G^{\ddagger}$, 51.64 ± 0.2 kJ mol^{-1}, $T_c = 253$ K).[11] The fluxional process producing this coalescence is clearly based on the flexibility of the boat conformation formed by the chelating aminophosphine. This phenomenon is well-known and has been studied for [RhCl(CO)(PN_1)], [Pd(Me)(OR)(PN_1)], and more recently $[Pt\{(o\text{-}Me_2Si)_2C_6H_4\}(PN_1)]$.[6,9,12]

For the (*R*)-P*N complex $[Rh(TFB)(P^*N)]BF_4$ (**3**), two conformers are observed at low temperature. At 203 K the $^{31}P\{^1H\}$ NMR spectrum displays two signals in the propor-

(5) (a) Casares, J. A.; Espinet, P.; Soulantica, K.; Pascual, I.; Orpen, A. G. *Inorg. Chem.* **1997**, *36*, 5251. (b) Alonso, M. A.; Casares, J. A.; Espinet, P.; Soulantica, K. Charmant, J. P. H.; Orpen, A. G. *Inorg. Chem*. **2000**, *39*, 705. (c) Casares, J. A.; Espinet, P.; Martín-Álvarez, J.; Espino, G.; Pérez-Manrique, M.; Vattier, F. *Eur. J. Inorg. Chem*. **2001**, 289. (d) Espinet, P.; Soulantica, K. *Coord. Chem. Rev*. **1999**, 499−556. (e) Zhang, Z. Z.; Cheng, H. *Coord. Chem. Rev*. **1996**, *147*, 1−39. (f) Newkome, G. R. *Chem. Rev*. **1993,** *93*, 2067−2089.
(6) Rauchfuss, T. B.; Patino, F. T.; Roundhill, D. M. *Inorg. Chem*. **1975**, *14*, 652.
(7) Garrou, P. E. *Chem. Rev*. **1981**, *81*, 229.
(8) Pregosin, P. S. *Phosphorus-31 NMR Spectroscopy in Stereochemical Analysis*; Verkade, J.-G., Quin, L. D., Eds.; VCH: Deerfield Beach, FL. 1987; Vol. 8, p 465 and references therein.
(9) Kapteijn, G. M.; Spee, M. P. R.; Grove, D. M.; Kooijman, H.; Spek, A. L.; van Koten, G. *Organometallics* **1996**, *15*, 1405.
(10) (a) Yang, H.; Lugan, N.; Mathieu, R. *Organometallics* **1997**, *16*, 2089. (b) Denise, B.; Pannetier, G. *J. Organomet. Chem.* **1978**, *148*, 155.
(11) Sandström J. *Dynamic NMR Spectroscopy*; Academic Press: London, 1982.
(12) Pfeiffer, J.; Kickelbick, G.; Schubert, U. *Organometallics* **2000**, *19*, 62.

Scheme 3. Schematic Representation for the Major Isomer of the Complexes [Rh(TFB)(P*N_n)]BF_4 (**3**) and Newman Projection along the C*−N Bond[a]

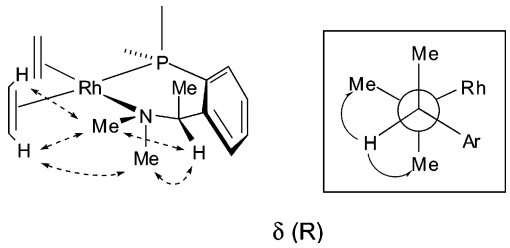

δ (R)

[a] The arrows indicate the most important NOE contacts between protons that were used for determining the conformation of the major isomer.

Chart 2

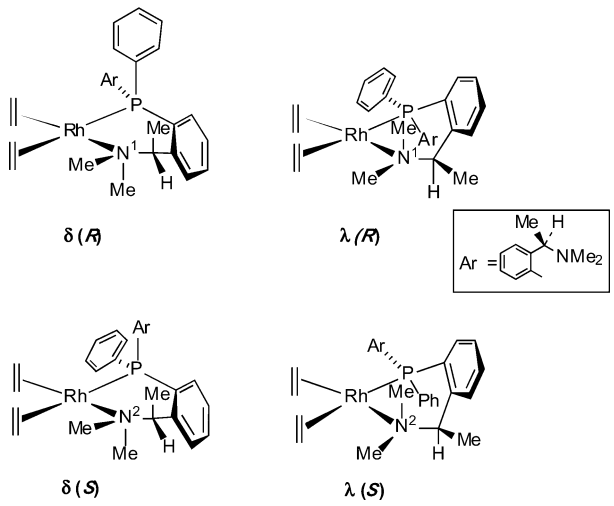

tion 10:1, at 24.4 and 25.5 ppm, respectively ($^1J_{Rh-P}$ = 174 Hz for both). The signals for two conformers are also seen in the ^{1}H NMR spectrum recorded under the same conditions. The major conformer shows six nonequivalent signals for the TFB ligand as well as the nonequivalence of the *N*-methyl groups. A NOESY experiment allows us to establish the conformation of the metallacycle in the major isomer as *δ* (NOE contacts are shown in Scheme 3). The ^{19}F NMR data are in agreement with the ^{31}P{^{1}H} and ^{1}H results. The minor isomer has the corresponding *λ* conformation, although not all the signals can be observed distinctly in the ^{1}H and NOESY spectra.

(b) Rhodium−PN_2−Diolefin and Rhodium−P*N_2−Diolefin Complexes. The coordination of the ligand PN_2 through the phosphorus and only one nitrogen renders nonequivalent the coordinated and the uncoordinated amino groups and converts the phosphorus atom to a chiral center (*R* or *S*). Therefore chelation by P*N_2 can give rise to four diastereoisomers *δ*(*R*), *λ*(*S*), *δ*(*S*), and *λ*(*R*) of different energies (Chart 2).

The complex [Rh(COD)(PN_2)]BF_4 (**4**) exists as one conformer according to their ^{31}P{^{1}H} and ^{1}H spectra. The NOE effect observed between the noncoordinated benzylamino group and the diolefin allows us to conclude that the P,N-ligand adopts a boat conformation with the free benzylamino group occupying an axial site (Scheme 4). The diagonal phase of the NOESY experiment (EXSY spectrum) shows cross peaks due to the exchange between free and

Scheme 4. NOE Contacts for Complex **4**

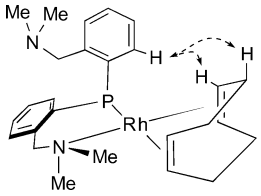

coordinated benzylamino group, both in the N(CH_3)$_2$ signals and in the benzylic groups. Exchange of the protons in the diolefin can also be observed in the cross peaks correlating endo−exo (relative to the boat) olefinic protons.

For [Rh(TFB)(PN_2)]BF_4 (**5**) an equilibrium between the two diastereomeric boat conformers exists in solution. At 213 K, ^{31}P{^{1}H}, ^{1}H, and ^{19}F spectra show two compounds in proportion 33:1. The rate of conformational exchange was calculated from the coalescence of these signals at 242 K, using spectra simulation.[13] The value obtained is $k_{major-minor}$ = 300 s^{-1} and corresponds to $\Delta G^{\ddagger}_{242} = 47.2 \pm 0.2$ kJ mol^{-1}. Furthermore, exchange of amino groups was observed in solution, which renders equivalent the olefinic protons of the TFB ligands. The rate of this process has been measured at the coalescence temperature of olefinic signal cis to nitrogen, giving a value of $\Delta G^{\ddagger}_{211} = 41.7 \pm 0.2$ kJ mol^{-1}.

Another interesting example of conformational analysis concerns the homologous complex [Rh(TFB)(P*N_2)]BF_4 (**6**). For a square planar geometry of Rh, coordination of the ligand can create two different isomers (depending on which amino group is coordinated), and each one can adopt two different conformations (Chart 2). The ^{31}P{^{1}H} NMR shows the existence of two compounds in approximately 10:1 proportion, at 26.1 ppm ($^1J_{Rh-P}$ = 172 Hz) and 31.2 ppm ($^1J_{Rh-P}$ = 170 Hz). In agreement with the ^{31}P results, the ^{19}F spectrum in $CDCl_3$ at 263 K shows two compounds in the same proportion (10:1), corresponding to a mixture of the two isomers in equilibrium. According to the ^{1}H NOE results, the major complex can be assigned as *δ* (*R*) (again the most important NOE interactions found are as indicated in Scheme 3). The ^{1}H NMR spectrum of *δ* (*R*) at 253 K (300.16 MHz) shows six nonequivalent protons for the TFB ligand, two complex signals attributable to the benzylic protons of the diamino arms (coordinated and noncoordinated), and two doublets for the *C**-methyl group (coordinated and noncoordinated). Also, two signals for the NMe_2 groups of the amine coordinated and one for the noncoordinated are observed. Assignment of the proton signals for the major isomer of **6** was possible using COSY and NOESY experiments. The correlation between the NMe_2 groups of the coordinated amino unit and the olefinic protons (at 5.8 and 5.4 ppm, which confirms their assignment to the protons trans to P), as well as with the benzylic proton, proves that the major isomer has a P,N-chelate ring in a twisted-boat conformation, with an absolute configuration *δ* and an axial *C**-methyl group (Chart 2). Furthermore, strong NOEs also occur between one of the methyl groups of the coordinated

(13) Line shape analysis was carried out using the standard DNMR 6 program: DNMR6. *Quantum Chemical Program Exchange (QCPE 633)*; Indiana University: Bloomington, IN, 1995.

Scheme 5

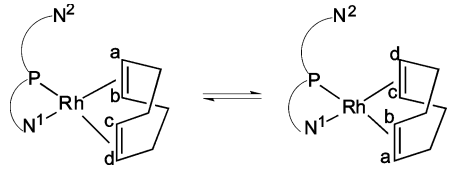

amino moiety and the C−H proton of the pendant phenylethylamine end. A correlation between the *C*-methyl group of the noncoordinated amino group and olefinic protons cis to N can also be observed. Altogether the evidence indicates that the major isomer is the δ form with an *R* configuration for the chiral phosphorus atom. In the complexes with PN_2 (**4** and **5**) the configuration found at the phosphorus was the opposite, with the noncoordinated benzylic amine in an axial position. Thus the configuration found in **6** is controlled by the *C*-methyl stereocenter in the chelate. Note that there is another possible stereoisomer in which both the *C*-methyl and the noncoordinated benzylamine group are in axial position (stereoisomer δ(S) in Chart 2), but this geometry maximizes the steric hindrance on this face of the chelating ring.

The EXSY spectrum of **6** shows cross peaks correlating the *N*-Me groups of the coordinated nitrogen of the major isomer and the $N(Me)_2$ of the free nitrogen in the minor one (a similar exchange was observed between the signal corresponding to the substituents of the α-carbon free and coordinated). The process involved is a substitution reaction with exchange of the uncoordinated and coordinated amines. The reaction equilibrates isomers with opposite absolute configuration at the phosphorus atom, *R* or *S*. On the other hand, at 263 K interconversion of the olefinic protons was observed. These data indicate the occurrence of a dynamic process that selectively exchanges the two olefinic protons trans to P with those trans to N (Scheme 5). This process is often observed in Rh(I)−diolefin complexes. It has been proposed to occur by a Berry mechanism in pentacoordinated intermediates formed by coordination of coordinating solvents or anions such as BF_4^-.[14] Other authors propose a different mechanism involving intermediates with a monodentate P,N-ligand.[15] The first step would involve Rh−N cleavage to form a three-coordinated species. Topomerization of the T-shaped intermediate is followed by rotation around the Rh−P bond and N recoordination. These mechanisms are indistinguishable by NMR experiments. In our complexes the exchange rate follows the order $PN_1 > PN_2 > PN_3$, and this excludes the intervention of the pendant amine groups to give a pentacoordinated intermediate, since in such a case the ligand with two pendant amino groups should be the fastest. Moreover, we have previously measured this process for diene complexes with the ligand PN_3 and it is very slow compared to the exchange under discussion here.[16] A dissociative pathway should be favored for the complex with the higher steric hindrance ($PN_3 > PN_2 > PN_1$), again in contrast with the observation. For this reason we favor an associative pathway involving solvent or the anion as the entering ligand.

Chart 3. Representation of the Two Conformers Observed for the Complex $[Rh(TFB)(P^*N_3)]BF_4$ (**7**)

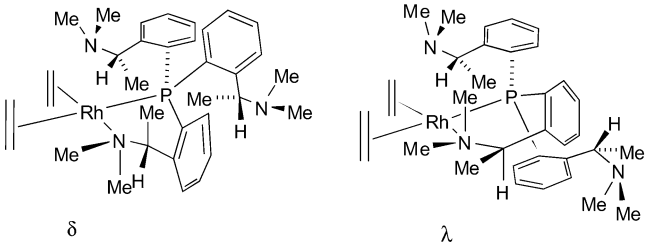

(c) Rhodium−PN_3−Diolefin and Rhodium−P^*N_3−Diolefin Complexes. We have reported previously the dynamic behavior of diene complexes with the ligand PN_3.[16] The Rh complexes are square planar in solution and undergo two intramolecular fluxional processes: conformational inversion and exchange of coordinated for the pendant amino groups. EXSY and magnetization transfer experiments demonstrated that both processes are not simultaneous but, on the contrary, the ligand exchange is ca. 100 times faster than the conformational change.

The complex with P^*N_3 behaves similarly to the analogous complex with P*N. The only difference between them is the steric hindrance around phosphorus. $^{31}P\{^1H\}$ and ^1H NMR spectra at 263 K show two conformers in equilibrium in the proportion 4:1 (Chart 3). The COSY and NOESY data confirm that the chelate has δ conformation in the major isomer. The assignments based on NOE contacts are as for P^*N_1 (Scheme 3).

Several dynamic processes were observed in the EXSY spectra of **7** at 263 K. For the major conformer we detected the following: (i) All of the methyls of the amino groups, whether coordinated or not, exchange with each other. The same applies with the CHMe groups. (ii) The double bonds exchange their coordination as a result of rotation of TFB ligand (Scheme 5). Furthermore, at the same temperature the experiment shows that conformer interconversion is occurring. The spectrum shows cross peaks correlating CHMe groups of the major isomer with others in the minor isomer. Although not every exchange can be observed in the complex spectrum, it can be seen clearly that the *C**-Me group of the coordinated amino arm of the major isomer and the *C**-Me signal of the pendant amine arm in the minor isomer do exchange. Therefore, overall the difference between rates of conformational inversion and rates of ligand substitution is smaller here than in the homologous complex with the nonchiral PN_3 (**9**, see Experimental Section).

X-ray Structure of Complex (8). Compound **8**, $[Rh(TFB)\{(C_6H_4CHMeNMe_2)_2P(C_6H_4CHMeNHMe_2)\}](BF_4)_2 \cdot H_2O \cdot Me_2CO$, was obtained as a decomposition product when we tried to obtain single crystals of $[Rh(TFB)(P^*N_3)]BF_4$

(14) (a) Haarman, H. F.; Ernsting, J. M.; Kranenburg, M.; Kooijman, H.; Veldamn, N.; Spek, A. L.; van Leeuwen, P. W. N. M. *Organometallics* **1997**, *16*, 887. (b) Heitner, H. I.; Lippard, S. J. *Inorg. Chem.* **1972**, *11*, 1447. (c) Vrieze, K.; van Leeuwen, P. W. N. M. Prog. *Inorg. Chem.* **1971**, *14*, 1. (d) Heitner, H. I.; Lippard, S. J. *J. Am. Chem. Soc.* **1970**, *92*, 3486.

(15) (a) Berger, H.; Nesper, R.; Pregosin, P. S.; Rüegger, H.; Wörle, M. *Helv. Chim. Acta* **1993**, *76*, 1520. (b) Yang, H.; Lugan, N.; Mathieu, R. *Organometallics* **1997**, *16*, 2089. (c) Selvakumar, K.; Valentini, M.; Pregosin, P. S. *Organometallics* **2000**, *19*, 1299.

(16) Alonso, M. A.; Casares, J. A.; Espinet, P.; Soulantica, K. *Angew. Chem., Int. Ed.* **1999**, *38*, 533.

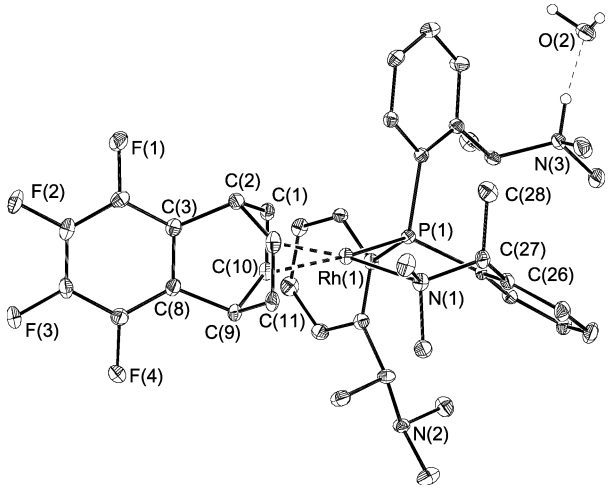

Figure 1. Thermal ellipsoid plot of the dication of [Rh(TFB){(C_6H_4-$CHMeNMe_2$)$_2$P($C_6H_4CHMeNHMe_2$)}](BF_4)$_2$·H_2O·Me_2CO and the water molecule to which it is hydrogen bonded. Ellipsoids are shown at the 40% probability level.

Table 1. Selected Bond Lengths (Å) and Angles (deg) for **8**

Rh(1)−C(10)	2.133(3)	Rh(1)−C(12)	2.250(3)
Rh(1)−C(1)	2.144(3)	Rh(1)−P(1)	2.3035(8)
Rh(1)−N(1)	2.176(2)	P(1)−C(31)	1.830(3)
Rh(1)−C(11)	2.246(3)		
C(10)−Rh(1)−C(1)	38.03(11)	N(1)−Rh(1)−C(12)	101.14(11)
C(10)−Rh(1)−N(1)	155.06(10)	C(11)−Rh(1)−C(12)	35.66(10)
C(1)−Rh(1)−N(1)	161.08(10)	C(10)−Rh(1)−P(1)	97.67(8)
C(10)−Rh(1)−C(11)	64.91(12)	C(1)−Rh(1)−P(1)	98.73(8)
C(1)−Rh(1)−C(11)	76.90(13)	N(1)−Rh(1)−P(1)	92.23(7)
N(1)−Rh(1)−C(11)	98.60(12)	C(11)−Rh(1)−P(1)	157.16(8)
C(10)−Rh(1)−C(12)	76.68(12)	C(12)−Rh(1)−P(1)	159.25(9)
C(1)−Rh(1)−C(12)	64.41(12)		

(**7**). The molecular structure of the dication and the associated hydrogen-bonded water molecule is shown in Figure 1. Table 1 contains a selection of bond distances and angles of interest.

The structure belongs to the monoclinic system with space group $P2_1$ and contains only the enantiomer shown in Figure 1 of the [Rh(TFB){P($C_6H_4CHMeNMe_2$)$_2$(C_6H_4CH-$MeNHMe_2$)}] dication together with BF_4^- anions and water and acetone molecules.

The dication of **8** contains a pseudo-square-planar rhodium bonded to the phosphorus and a nitrogen atom of the bidentate protonated P($C_6H_4CHMeNMe_2$)$_2$(C_6H_4CH-$MeNHMe_2$) ligand (PN*$_3$H$^+$) and to the olefinic bonds of a tetrafluorobenzobarrelene (TFB) ligand. The TFB ligand shows no peculiar structural features and has Rh−C bond distances similar to those in other such complexes.[17,18] Coordination of the TFB leads to C−Rh−C angles well below 90°, as expected for its small bite angle. The P−Rh−N(1) angle, however, is close to 90°. The Rh−P and Rh−N distances are within the normal ranges for Rh(I) complexes.[19]

The Rh−C bond lengths reflect the stronger trans influence of the phosphine compared with the tertiary amine. The structure features a six-membered metallacycle, Rh−P(1)−C(21)−C(26)−C(27)−N(1) with a twisted-boat conformation of absolute configuration δ and with the C(28) methyl group in an axial site. The protonated amino group occupies a pseudo-axial position and is hydrogen bonded to the water molecule (see Figure 1).

Complex **8** could not be prepared by the reaction between **7** and aqueous HBF_4 in which extensive decomposition occurred. However, the protonation of **7** by H(OEt_2)$_2$BAF (BAF: tetrakis[3,5-bis(trifluoromethyl)phenyl]borate) in an NMR tube allowed us to complete the spectroscopic characterization of the dication of **8**, [Rh(TFB){(C_6H_4CHMe-NMe_2)$_2$P($C_6H_4CHMeNHMe_2$)}]$^{2+}$.

Discussion

Conformational Preferences in the Solid State and in Solution. The twisted-boat conformation of the metallacycles formed by the chelating ligands in this work is chiral and exists in δ and λ forms.[20] Solid state structures of transition metal complexes (e.g., Rh, Pd, Pt, Ni) with ligands closely related to ours have been reported and confirm that the preferred conformation is related to the configuration of the α-carbon stereocenter. For example, this is observed in Rh complexes with (*R*)-*N*,*N*-dimethyl-1-phenylethylamine, [(1*R*)-*N*,*N*-dimethyl{*o*-[bis-*tert*-butylphosphino]phenyl}ethylamine-*N*,*P*],[21] or (*R*,*S*)-α-(2-diphenylphosphinoferrocenyl)ethyldimethylamine,[22] and in the Ni complex [Ni{(*R*)-*o*-(C_6H_{11})$_2$-$PC_6H_4CHCH_3N(CH_3)_2$}(NCS)$_2$].[23] On the contrary, when the configuration of the carbon stereocenter is *S*, the P,N-chelate ring presents a twisted-boat conformation with an absolute configuration λ and an axial *C*-methyl group. This is observed in the Rh complexes with (*S*,*S*)-bis[2-(1-*N*,*N*-dimethylaminoethyl)phenyl]phenyl)phosphine or (*S*)-[2-(1-*N*,*N*-dimethylaminoethyl)phenyl]diphenylarsine,[21] and in the structure of *cis*-dichloro[(1*S*)-*N*,*N*-dimethyl-1-{2-[(*S*)-*tert*-butylphenylphosphino]phenyl}ethylamine-*N*,*P*]platinum-(II).[24] In conclusion, for *R* α-carbon stereocenters the six-membered ring adopts the conformation δ, and for *S* α-carbon stereocenters the conformation will be λ.

Similarly for the P*N$_n$ ligands the preferred conformation of the metallacycle is that minimizing the steric interactions between the methyl substituent and those on the N atom,[25−27] and the δ configuration will be expected for the chelate ring

(17) (a) Lahoz, F. J.; Tiripicchio, A.; Camellini, T. M.; Oro, L. A.; Pinillos, M. T. *J. Chem. Soc., Dalton Trans.* **1985**, 1487. (b) Ciriano, M. A.; Perez-Torrente, J. J.; Viguri, F.; Lahoz, F. J.; Oro, L. A.; Tiripicchio, A.; Camellini, T. M. *J. Chem. Soc., Dalton Trans.* **1990**, 1493. (c) Esteruelas, M. A.; Lahoz, F. J.; Oliván, M.; Oñate, E.; Oro, L. A. *Organometallics* **1994**, *13*, 3315. (d) Atencio, R.; Casado, M. A.; Ciriano, M. A.; Lahoz, F. J.; Perez-Torrente, J. J.; Tiripicchio, A.; Oro, L. A. *J. Organomet. Chem.* **1996**, *514*, 103.

(18) Esteruelas, M. A.; Oro, L. A. *Coord. Chem. Rev.* **1999**, *193*−*195*, 557.

(19) Orpen, A. G.; Brammer, L.; Allen, F. H.; Kennard, O.; Watson, D. G.; Taylor, R. *J. Chem. Soc., Dalton Trans.* **1989**, S1−S83.

(20) Eliel, E. L.; Wilen, S. H. *Stereochemistry of Organic Compounds*; John Wiley & Sons: New York, 1994.

(21) McKay, I. D.; Payne, N. *Can. J. Chem.* **1986**, *64*, 1930.

(22) Cullen, W. R.; Eisentein, F. W. B.; Huang, C.-H.; Willis, A. C.; San Yeh, E. *J. Am. Chem. Soc.* **1980**, *102*, 988.

(23) McKay, I. D.; Payne, N. C. *Acta Crystallogr., Sect. C: Cryst. Struct. Commun.* **1986**, *42*, 307.

(24) Payne, N. C.; Tobin, G. R. *Acta Crystallogr.* **1992**, *C48*, 45.

(25) Yamada, I.; Ohkouchi, M.; Yamaguchi, M.; Yamagishi, T. *J. Chem. Soc., Perkin Trans. 1* **1997**, 1869.

(26) Payne, N.; Stephan, D. W. *Inorg. Chem.* **1982**, *21*, 182.

(27) Chooi, S. Y. M.; Leung, P. H.; Mok, K. F. *Inorg. Chem.* **1994**, *33*, 3096.

Chart 4. Schematic Representations of δ and λ Twisted-Boat Conformations (for (*R*)-*C**-Me Stereocenter), Showing the Overlap of the Me Groups in the λ Conformer

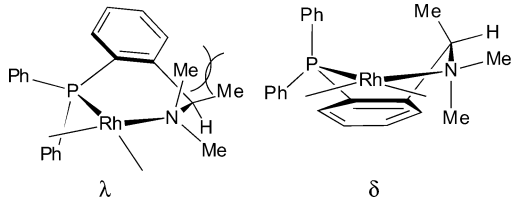

Table 2. Selected Values of Activation Energies for the Conformational Inversion of the Ligand PN_1

complexes	$\Delta G^{\ddagger}$ (kJ mol^{-1})	T_c (K)	ref
[RhCl(CO)(PN_1)]	36.66	221	6
[Pd(Me)($OCH(CF_3)_2$(PN_1)]	41.66	215[a]	9
[Pd(Me)(OC_6H_5)(PN_1)]	41.66	215[a]	9
[Pt(*o*-$Me_2Si(C_6H_4)$)(PN_1)]	51.00	266	12
[Pt($Me)_2$(PN_1)]	55.00	276	12
[PtI(Me)(PN_1)]	57.00	289	12
[Rh(TFB)(PN_1)]BF_4	41.52	211	this work
[Rh(COD)(PN_1)]BF_4	51.64	253	this work

[a] The coalescence temperature for these complexes was not reported and has been calculated from the reported $\Delta\delta$ and $\Delta G^{\ddagger}$ values.

when the absolute configuration of the carbon stereocenter is *R*. This is in fact the configuration observed in the structure of **8**.

In solution we can observe this conformational preference for the complexes **3**, **6**, and **7**. In fact the variable-temperature $^{31}P\{^1H\}$ and ^1H NMR spectra show the two conformers in equilibrium, but the preferred one is always very dominant (**3** 100:3, **6** 10:1, **7** 4:1). This conformation is independent of the steric hindrance around the phosphorus center. The preference observed for coordinated P,N-ligands agrees with that suggested even by simple ball-and-stick models, which suggest severe steric repulsions between the methyl on the α-carbon and the equatorial methyl of the *syn*-amine group in the $\lambda(R)$ conformation (Chart 4). This steric repulsion disappears in the δ configuration. This probably dictates the conformational preference observed.

Dynamic Behavior in Solution. The complexes reported here show at least two dynamic processes in solution: (i) inversion of the conformation of the nonplanar metallacycle and (ii) exchange of amino groups, which depends on the geometrical restrictions around phosphorus, the stereogenic centers, and the corresponding diolefin ligands.

Conformational Exchange. The complexes with PN_1, [Rh(TFB)(PN_1)]BF_4 (**1**) and [Rh(COD)(PN)]BF_4 (**2**), are involved in a fast conformational inversion of the metallacycle formed by the chelating ligand, which is plane-averaged on the NMR time scale. Table 2 gathers the activation free energy for **1** and for **2** along with other values reported in the literature. The wide range of variation does not permit one to establish meaningful comparisons.

If we compare the complexes with ligands PN_1 (with two Ph pendant groups) with those with PN_3 (having two benzylamino pendant groups), we observe that an increase in the number of benzylamine groups leads to a slower conformational inversion. For PN_2 the pendant substituents of phosphorus are different from each other (one Ph and one benzylamino), and this is a factor that leads to very different energies for the conformational isomers, making any comparison of boat-exchange energies difficult.

However, it is very interesting to note that, in the homologous complexes with P*N_n (where the ligands have a Me group as the α-carbon substituent), the conformational inversion rates decrease considerably. For instance the conformational inversion for the complex [Rh(TFB)(P*N_1)]BF_4 (**3**) is so slow that the coalescence in acetone-d_6 of the olefin signals of the major with those of the minor isomer is above room temperature, whereas for [Rh(TFB)(PN_1)]BF_4 (**1**) the coalescence temperature is 213 K. Therefore an important effect of the *C*-Me substituent in the P*N_n ligands is to increase the activation energy for the exchange between the two conformers. These results are in agreement with the work of Crociani et al. on the influence of steric factors on ring inversion observed for iminophosphine−rhodium derivatives.[4f]

Exchange of Amino Groups. Exchange of pendant and coordinated amino groups was observed for the PN_2 complexes **5** and **4** and is thought to occur by an associative mechanism, which requires the formation of pentacoordinated species. In fact the rate of substitution is moderately faster for **5** than **4**, as expected if we consider that the stabilization of the transition state is bigger for the TFB complex (stronger π-back-bonding due to the strained chelate formed) than for the COD complex. The same fluxional behavior is observed for the compounds with the PN_3 ligands (**9** and **10**, see Experimental Section). The exchange observed is slightly slower than for the homologous complex with PN_2, likely due to the increase in the relative steric crowding around phosphorus. As for the conformational inversion, the *C*-Me substituent in complexes with P*N_n ligands increases the activation energy associated with the exchange of amino groups.

Finally, it is remarkable that the relative difference in rates of substitution is lower between complexes with P*N_2 and P*N_3 than for the couple PN_2 and PN_3. This reflects that the steric effect of *C*-Me substituents is more important than the increase of the steric crowding.

Experimental Section

General Methods. All reactions were carried out under N_2 using standard Schlenk techniques. Solvents were distilled using standard procedures and degassed under nitrogen before use. The precursors [$Rh_2(\mu$-Cl)$_2$(1,5-COD)$_2$],[28] [$Rh_2(\mu$-Cl)$_2$(TFB)$_2$],[29] the ligands PN_3,[30] P*N,[31] and P*N_2,[32] and $TlBF_4$ were prepared by published methods.[33] Combustion CHN analyses were made on a Perkin-Elmer 2400 CHN microanalyzer. Optical rotations were measured with a Perkin-Elmer 241 polarimeter using 10-cm cells. ^1H NMR (300.16 MHz), ^{19}F NMR (282.4 MHz), $^{31}P\{^1H\}$ NMR (121.4 MHz), and $^{13}C\{^1H\}$ (75.47 MHz) spectra were recorded on Bruker ARX 300 and AC 300 instruments equipped with a VT-100 variable-

(28) Giordano, G.; Crabtree, R. H. *Inorg. Synth.* **1990**, *28*, 88.
(29) Roe, D. M.; Massey, A. G. *J. Organomet. Chem.* **1971**, *28*, 273.
(30) Chuit, C.; Corrin, J. P. R.; Monforte, P.; Reyé, C.; Declereq, J.-P.; Duborg, A. *Angew. Chem., Int. Ed. Engl.* **1993**, *32*, 1430.
(31) Horner, L.; Simons, G. *Phosphorus Sulfur Relat. Elem.* **1983**, *15*, 171.
(32) Yamada, I.; Ohkouchi, M.; Yamaguchi, M.; Yamagishi, T. *J. Chem. Soc., Perkin Trans. 1* **1997**, 1869.
(33) Arnáiz, J. *J. Chem. Educ.* **1997**, *74*, 1332.

temperature probe. Chemical shifts are reported in parts per million from tetramethylsilane for ^{1}H and ^{13}C; CCl_3F for ^{19}F; and H_3PO_4 (85%) for ^{31}P; positive shifts downfield at ambient probe temperature unless otherwise stated. NOESY experiments were recorded in phase sensitive mode, using the average of the relaxation times as mixing time.

[(2-*N*,*N*-Dimethylaminomethyl)phenyl]diphenylphosphine (PN$_1$). This ligand, first prepared by Roundhill et al., was synthesized according to the published method[6] with minor modifications. To a solution of BuLi (26 mL, 42 mmol) in hexane (40 mL), prepared by dilution of a commercial solution (1.6 M in hexane), were added ether (30 mL) and *N*,*N*-dimethylbenzylamine (6 mL, 40 mmol) just after, and the mixture was refluxed for 5 h. This orange solution was cooled −78 °C and a solution of freshly distilled Ph_2PCl (6.47 mL, 36 mmol), in ether (20 mL) was added slowly during 1 h. This mixture was allowed to react at low temperature overnight, and then the solvent was evaporated and the excess of lithium salts hydrolyzed by adding ethanol (3 mL) and then water (30 mL). The phosphine was extracted with dichloromethane (90 mL in three portions), dried with magnesium sulfate, and concentrated to dryness. The product was crystallized by adding ethanol (25 mL) and cooling at −20 °C. Yield: 9.2 g (90%).

Bis[(2-*N*,*N*-Dimethylaminomethyl)phenyl]phenylphosphine (PN$_2$). The procedure was as described for PN, but $PhPCl_2$ (2.2 mL, 17 mmol) was added instead of Ph_2PCl. The crude product was purified by column chromatography on silica gel using ethyl acetate as eluent Yield: 4.09 g (64%). Anal. Calcd for $C_{24}H_{29}N_2P$: C, 76.75; H, 7.76; N, 7.44. Found: C, 76.73; H, 7.35; N, 7.71. ^{31}P{^{1}H} NMR ($CDCl_3$, 25 °C): δ −24.70 s. ^{1}H NMR ($CDCl_3$, 25 °C): δ 7.48 (ddd, J_{56} = 4.2 Hz, J_{53} = 1.25 Hz, J_{54} = 7.6 Hz, 2*H*$_5$), δ 7.32 (m, 5H, Ph), δ 7.20 (m, 2*H*$_3$), δ 7.12 (td, J_{43} = 7.45 Hz, J_{45} = 7.6 Hz, J_{46} = 1.22 Hz, 2*H*$_4$), δ 6.82 (dd, J_{H-P} = 6.8 Hz, J_{65} = 4.2 Hz, 2*H*$_6$), δ 3.60 (system ABX, 4H, C*H*$_2$), δ 2.18 (s, 12H, N(C*H*$_3$)$_2$). ^{13}C{^{1}H} NMR ($CDCl_3$, 25 °C): δ 144.13 (d, J_{C-P} = 22.6 Hz, *C*H), δ 138.51 (d, J_{C-P} = 10.5 Hz, *C*H), δ 137.51 (d, J_{C-P} = 13.5 Hz, *C*H), δ 134.69 (s, *C*H), δ 134.50 (s, *C*H), δ 134.42 (s, *C*H), δ 129.49 (d, J_{C-P} = 9.8 Hz, *C*H), δ 128.94 (s, *C*H), δ 128.87 (s, *C*H), δ 128.74 (d, J_{C-P} = 5.3 Hz, *C*H), δ 127.45 (s, *C*H), δ 62.61 (d, J_{C-P} = 19.6 Hz, *C*H$_2$), δ 45.65 (s, *C*H$_3$).

(*R*,*R*,*R*)-Tris-[2-(1-*N*,*N*-dimethylaminoethyl)phenyl]phosphine (P*N$_3$). To a solution of BuLi (9 mL, 14 mmol) in hexane (15 mL), prepared by dilution of a commercial solution (1.6 M in hexane), were added tetraethylenediamine (2.1 mL, 14 mmol) and (*R*)-(+)-α-*N*,*N*-dimethyl-1-phenylethylamine (2 g, 13 mmol) just after, and the mixture was refluxed for 5 h. This orange solution was added slowly during 1 h to a solution of freshly distilled PCl_3 (0.3 mL, 3 mmol), in ether (10 mL). This mixture was allowed to react at low temperature overnight, and then the excess of lithium salts was hydrolyzed by adding a solution of saturated sodium carbonate (25 mL). The phosphine was extracted with ether (30 mL in three portions), dried with magnesium sulfate, and concentrated to dryness. The phosphine was crystallized by adding acetonitrile. Yield: 340 mg (47%). Anal. Calcd for $C_{30}H_{42}N_3P$: C, 75.75; H, 8.90; N, 8.83. Found: C, 75.15; H, 8.49; N, 8.20. Optical rotation: $[\alpha]_D^{20}$ = +122.6 (*c* = 1, in $CDCl_3$). ^{31}P{^{1}H} NMR ($CDCl_3$, 25 °C): δ −42.97 s. ^{1}H NMR ($CDCl_3$, 25 °C): δ 7.58 (dd, *J* = 6.7 Hz, *J* = 4.4 Hz, 3H, H$_6$), δ 7.35 (t, *J* = 7.2 Hz, 3H, H$_5$), δ 7.11 (t, *J* = 7.3 Hz, 3H, H$_4$), δ 6.75 (br, 3H, H$_3$), δ 4.07 (br, 3H, C*H*Me), δ 2.28 (br, 18H, N(C*H*$_3$)$_2$), δ 0.95 (a, 9H, CH*Me*). ^{13}C{^{1}H} NMR ($CDCl_3$, 25 °C): δ 149.80 (d, J_{C-P} = 21.3 Hz, *C*H), δ 134.48 (d, J_{C-P} = 11 Hz, *C*H), δ 129.31 (s, *C*H), δ 126.71 (s, *C*H), 115.16 (d, J_{C-P} = 5 Hz, *C*H), 61.83 (s, *C*H), 43.99 (s, *C*H$_3$), 21.11 (s, *C*H$_3$).

[Rh(TFB)(PN)]BF$_4$ (1). To a stirred suspension of [Rh$_2$(μ-Cl)$_2$(TFB)$_2$] (248 mg, 0.34 mmol) in acetone (20 mL) were added solid PN (217 mg, 0.68 mmol) and $TlBF_4$ (198 mg, 0.68 mmol). After 1 h the TlCl was removed by filtration. The yellow solution was concentrated to 10 mL, and after addition of ethanol (10 mL) it was allowed to crystallize. The bright yellow crystals formed were washed with ethanol and dried under vacuum. Yield: 342 mg (68%). Anal. Calcd for $C_{33}H_{28}BF_8NPRh$: C, 53.91; H, 3.84; N, 1.91. Found: C, 54.47; H, 1.93; N, 4.04. ^{31}P{^{1}H} NMR (CD_2Cl_2, 25 °C): δ 30.88 (d, J_{Rh-P} = 174.4 Hz). ^{1}H NMR (CD_2Cl_2, 25 °C): δ 7.00−7.70 (m, 10H, Ar), δ 7.32 (m, 3H, Ar), δ 7.00 (m, 1H, Ar), δ 5.80 (br, 2H, *H*-Cbridge(TFB)), δ 5.10 (br, 2H, *Holef-cisN*(TFB)), δ 3.65 (m, 2H, *Holef-transN*(TFB)), δ 2.60 (s, 6H, NcoordC*H*$_3$ + NcoordC*H*$_3$). ^{19}F NMR (CD_2Cl_2, 25 °C): δ −159.04 (m, 2F), δ −146.33 (m, 2F), δ −152.19 (s, ^{10}B*F*$_4$), δ −152.25 (s, ^{11}B*F*$_4$).

[Rh(COD)(PN)](BF$_4$) (2). To a stirred solution of [Rh$_2$(μ-Cl)$_2$(COD)$_2$] (247 mg, 0.5 mmol) in acetone (30 mL) was added $AgBF_4$ (196 mg, 1 mmol). After half an hour, the AgCl was removed by filtration and solid PN (319 mg, 1 mmol) was added. The yellow solution was concentrated and cooled for crystallization to −20 °C for 1 day. The bright yellow crystalline solid was filtered, washed with acetone−ethanol (1:1), and dried in a vacuum. By concentration of the remaining solution a second crop of crystals was obtained. Yield: 525 mg (85%). Anal. Calcd for $C_{29}H_{34}BF_4NPRh$: C, 56.43; H, 5.55; N, 2.27. Found: C, 56.33; H, 5.64; N, 2.22. ^{31}P{^{1}H} NMR ($CDCl_3$, 213K): δ 25.05 (d, J_{Rh-P} = 156.9 Hz). ^{1}H NMR ($CDCl_3$, 213K): δ 8.08 (m, 1H, Ar), δ 7.8−7.0 (m, 13H, Ar), δ 5.75 (m, 1H, C*H*(COD)), δ 5.15 (m, 1H, C*H*(COD)), δ 3.78 (m, 1H, C*H*$_2$), δ 3.35 (m, 1H, C*H*$_2$), δ 3.20 (m, 2H, C*H*(COD)), δ 2.85 (m, 2H, C*H*$_2$(COD)), δ 2.68 (s, 3H, NcoordC*H*$_3$), δ 2.51 (s, 3H, NcoordC*H*$_3$), δ 2.39 (m, 3H, C*H*$_2$ (COD)), 1.97 (m, 2H, C*H*$_2$-(COD)), 1.65 (m, 1H, C*H*$_2$(COD)).

[Rh(TFB)(P*N)]BF$_4$ (3). This compound was prepared as described for **1**, but using (*R*)-P*N (225 mg, 0.68 mmol) instead of PN. Yield: 326 mg (64%). Anal. Calcd for $C_{34}H_{30}BF_8NPRh$: C, 54.50; H, 4.04; N, 1.87. Found: C, 54.22; H, 4.04; N, 1.80. Optical rotation: $[\alpha]_D^{20}$ = −64.8 (*c* = 0.95, in $CDCl_3$). ^{31}P{^{1}H} NMR ($CDCl_3$, 25 °C): δ 23.6 (d, J_{Rh-P} = 174 Hz). ^{31}P{^{1}H} NMR (CD_2Cl_2, −70 °C): δ 24.6 (d, major conformer J_{Rh-P} = 174 Hz); δ 25.4 (d, minor conformer J_{Rh-P} = 169 Hz). ^{1}H NMR ($CDCl_3$, 25 °C): δ 7.66 (m, 2H, Ar), 7.6−7.3 (m, 12H, Ar), δ 5.82 (m, 2H, *H*-Cbridge), δ 5.67 (m, 1H, *Holef-cisN* (TFB)), δ 5.53 (m, 1H, *Holef-cisN* (TFB)), δ 3.62 (m, 1H, C*H*Me), δ 3.22 (m, 1H, *Holef-transN* (TFB)), δ 3.10 (m, 1H, *Holef-transN* (TFB)), δ 2.72 (s, 6H, NcoordC*H*$_3$ + NcoordC*H*$_3$), δ 1.79 (d, *J* = 6.7 Hz, 3H, CH*Me*). ^{19}F NMR ($CDCl_3$, 25 °C): δ −145.76 (m, 1F), −146.28 (m, 1F), −152.43 (s, ^{10}B*F*$_4$), −152.49 (s, ^{11}B*F*$_4$), −158.95 (m, 2F).

[Rh(COD)(PN$_2$)](BF$_4$) (4). This compound was prepared as described for **2**, but using PN_2 (377 mg, 1 mmol) instead of PN. Yield: 587 mg (87%). Anal. Calcd for $C_{32}H_{41}BF_4N_2PRh$: C, 56.99; H, 6.13; N, 4.15. Found: C, 56.62; H, 6.16; N, 3.90. ^{31}P{^{1}H} NMR ($CDCl_3$, 233 K): δ 16.84 (d, J_{Rh-P} = 159.5 Hz). ^{1}H NMR ($CDCl_3$, 233 K): δ 9.20 (dd, *J* = 7.5 Hz, *J* = 13.5 Hz, 1H, Ar), δ 7.85 (m, 2H, Ar), δ 7.60 (m, 2H, Ar), δ 7.34, (m, 5H, Ar), δ 7.12 (m, 3H, Ar), δ 5.70 (m, 1H, C*H*(COD)), δ 5.31 (m, 1H, C*H*(COD)), δ 4.03 (d, *J* = 13.2 Hz, 1H, C*H*$_2$), δ 3.90 (d, *J* = 16.3 Hz, 1H, C*H*$_2$), δ 3.40 (m, 2H, C*H*$_2$ + C*H*(COD)), δ 3.20 (d, *J* = 15.6 Hz, 1H, C*H*$_2$), δ 2.98 (m, 1H, C*H*$_2$(COD)), δ 2.80 (s, 3H, NcoordC*H*$_3$), δ 2.75 (masked, 1H, C*H*$_2$(COD)), δ 2.55 (s, 3H, NcoordC*H*$_3$), δ 2.53 (m, 1H, C*H*$_2$(COD)), δ 2.40 (s, 3H, C*H*$_2$ (COD) + C*H*(COD)), δ 2.28 (s, 6H, N(C*H*$_3$)$_2$), δ 2.04−1.5 (m, 3H, C*H*$_2$(COD)).

[Rh(TFB)(PN$_2$)]BF$_4$ (5). This compound was prepared as described for **1**, but using PN_2 (256 mg, 0.68 mmol) instead of PN. Yield: 431 mg (80%). Anal. Calcd for $C_{36}H_{35}BF_8N_2PRh$: C, 54.57; H, 4.45; N, 3.54. Found: C, 54.38; H, 4.52; N, 3.41. ^{31}P-{^{1}H} NMR (CD_2Cl_2, 25 °C): δ 26.19 (d, J_{Rh-P} = 172.7 Hz). ^{31}P-{^{1}H} NMR (CD_2Cl_2, −90 °C): δ 24.2 (d, major conformer J_{Rh-P} = 172 Hz); 35.8 (d, minor conformer J_{Rh-P} = 173 Hz). ^{1}H NMR (CD_2Cl_2, 25 °C): δ 7.96 (br, 2H, Ar), δ 7.55−7.40 (m, 7H, Ar), δ 7.25 (m, 2H, Ar), δ 7.12 (m, 2H, Ar), δ 5.68 (br, 2H, *H*-Cbridge-(TFB)), δ 5.41 (br, 2H, *Holef-cisN*(TFB)), δ 3.45 (m, 4H, C*H*$_2$), δ 2.88 (br, 2H, *Holef-transN*(TFB)), δ 2.32 (br, 12H, N(C*H*$_3$)$_2$ + NcoordC*H*$_3$ + NcoordC*H*$_3$). ^{19}F NMR (CD_2Cl_2, 25 °C): δ −158.80 (m, 2F), δ −146.11 (m, 2F), δ −151.94 (s, ^{10}B*F*$_4$), δ −152.00 (s, ^{11}B*F*$_4$). ^{1}H (CD_2Cl_2, 183 K): δ 9.15 (m, 1H, Ph), δ 7.71 (m, 2H, Ph), δ 7.5−6.9 (m, 9H, Ph), δ 6.62 (m, 1H, Ph), δ 5.90 (br, 1H, *Holef-cisN*(TFB)), δ 5.60 (br, 1H, *H*-Cbridge(TFB)), δ 5.35 (br, 1H, *Holef-cisN*(TFB)), δ 5.17 (br, 1H, *H*-Cbridge(TFB)), δ 3.74 (m, 2H, C*H*$_2$), δ 3.28 (br, 2H, *Holef-transN*(TFB) + C*H*$_2$), δ 3.01 (br, 1H, C*H*$_2$), δ 2.54 (br, 3H, NcoordC*H*$_3$), δ 2.35 (br, 4H, NcoordC*H*$_3$ + *Holef-transN*(TFB)), δ 2.22 (br, 6H, N(C*H*$_3$)$_2$).

[Rh(TFB)(P*N$_2$)]BF$_4$ (6). This compound was prepared as described for **1**, but using (*R, R*)-P*N$_2$ (275 mg, 0.68 mmol) instead of PN. Yield: 502 mg (90%). Anal. Calcd for $C_{38}H_{39}BF_8N_2PRh$: C, 55.63; H, 4.79; N, 3.41. Found: C, 54.50; H, 5.11; N, 2.92. Optical rotation: $[\alpha]_D^{20}$ = −24.56 (c = 1.25, in $CDCl_3$). ^{31}P{^{1}H} NMR ($CDCl_3$, 25 °C): (a) major conformer, δ 26.13 (d, $^1J_{Rh-P}$ = 172.6 Hz); (b) minor conformer, δ 31.20 (d, $^1J_{Rh-P}$ = 169.9 Hz). ^{1}H NMR ($CDCl_3$, 25 °C): major conformer, δ 9.17 (br, 1H), 7.98−6.90 (mixture of conformers), δ 6.13 (br, 1H), δ 5.86 (br, 1 H), δ 5.45 (m, 2H), δ 3.52 (br, 2H), δ 3.25 (m, 1H), δ 2.77 (m, 6H), δ 2.13 (br, 1H), δ 2.03 (br, 6H), δ 1.96 (m, 3H), δ 1.40 (d, J = 6.7 Hz, 3H). ^{19}F NMR ($CDCl_3$, 25 °C): δ −145.76 (m, 1F), −146.28 (m, 1F), −152.19 (s, ^{10}B*F*$_4$), −152.49 (s, ^{11}B*F*$_4$), −158.95 (m, 2F). ^{1}H NMR ($CDCl_3$, 253K): major conformer: δ 9.15 (m, 1H, Ar), 7.9−6.9 (mixture of conformers), δ 6.13 (m, 1H, *H*-Cbridge(TFB)), δ 5.86 (m, 1H, *Holef-cisN* (TFB)), δ 5.42 (m, 1H, *Holef-cisN* (TFB)), δ 5.33 (m, 1H, *H*-Cbridge(TFB)), δ 3.52 (m, 2H, *Holef-transN* (TFB) + C*H*Mecoord), δ 3.11 (m, 1H, C*H*Me), δ 2.77 (s, 6H, NcoordC*H*$_3$), δ 2.68 (s, 3H, NcoordC*H*$_3$), δ 2.01 (m, 10H, N(C*H*$_3$)$_2$ + *Holef-transN* (TFB)+CH*Me*), δ 1.38 (d, J = 6.2 Hz, 3H, CH*Me*coord).

[Rh(TFB)(P*N$_3$)]BF$_4$·2H$_2$O (7). This compound was prepared as described for **1**, but using (*R,R,R*)-P*N$_3$ (322 mg, 0.68 mmol) instead of PN. Yield: 502 mg (81%). Anal. Calcd for $C_{42}H_{52}BF_8N_3O_2PRh$: C, 54.38; H, 5.65; N, 4.53. Found: C, 54.21; H, 5.28; N, 4.26. Optical rotation: $[\alpha]_D^{20}$ = −48.20 (c = 1, in $CDCl_3$). ^{31}P{^{1}H}NMR ($CDCl_3$, 25 °C): (a) major conformer, δ 36.8 (d, J_{Rh-P} = 171 Hz); (b) minor conformer, δ 34.3 (d, J_{Rh-P} = 182 Hz). ^{1}H NMR ($CDCl_3$, 25 °C): major conformer only, δ 10.29 (m, 1H, Ar), 8.00 (m, 2H, Ar), 7.90 (m, 1H, Ar), 7.7−7.5 (m, 2H, Ar), 7.5−7.4 (m, 3H, Ar), 7.47 (m, 1H, Ar), 7.08 (m, 1H, Ar), 6.65 (m, 1H, Ar), 6.02 (m, 1H, *H*-Cbridge(TFB)), 5.78 (m, 1H, *Holef-cisN* (TFB)), 5.37 (m, 1H, *H*-Cbridge(TFB)), 5.22 (m, 1H, *Holef-cisN* (TFB)), 3.81 (m, 1H, C*H*Me), 3.62 (m, 1H, C*H*Me), 3.50 (m, 1H, C*H*Mecoord), 3.11 (m, 1H, *Holef-transN* (TFB)), 2.61 (s, 3H, NcoordC*H*$_3$), 2.50 (s, 3H, NcoordC*H*$_3$), 2.12 (s, 6H, N(C*H*$_3$)$_2$), 1.83 (m, 1H, *Holef-transN* (TFB)), 1.71 (d, J = 6.5 Hz, 3H, CH*Me*), 1.43 (s, 6H, N(C*H*$_3$)$_2$), 1.22 (d, J = 6.4 Hz, 3H, CH*Me*), 1.15 (d, J = 6.9 Hz, 3H, CH*Me*coord). ^{19}F NMR ($CDCl_3$, 25 °C): δ −146.58 (m, 2F), −149.55 (s, ^{10}B*F*$_4$), −149.60 (s, ^{11}B*F*$_4$), −160.06 (m, 2F).

Protonation of 7. To a solution of 25 mg of **7** (0.028 mmol) in $CHCl_3$ (0.5 mL) was added 28 mg of H(OEt$_2$)$_2$BAF (0.028 mmol). A red oil precipitated immediately from the solution. The solvent was decanted, and the oil was washed with *n*-hexane, vacuum-dried, and dissolved in CD_2Cl_2 to obtain its spectroscopic data. ^{31}P-{^{1}H} NMR: δ 31.2 (d, J_{Rh-P} = 180 Hz). ^{1}H NMR: δ 14.3 (br, 1H, N−*H*), 9.70, (m, 1H), 8.2−6.6 (m, 11H), 5.87 (br, 1H, *TFB*), 5.55 (br, 1H, *TFB*), 5.48 (br, 1H, *TFB*), 5.06 (br, 1H, *TFB*), 4.30 (m, 1H, C*H*Me), 3.98 (m, 1H, C*H*Me), 3.52 (m, 1H, C*H*Me), 3.34 (br, 1H, *TFB*), 2.50 (br, 1H, *TFB*), 2.60 (s, 3H, N-*Me*), 2.45 (s, 6H, N-*Me*), 2.14 (s, 3H, N−*Me*), 1.88 (s, 3H, N−*Me*), 1.41 (s, 3H, N−*Me*), 1.16 (d, J = 6.7 Hz, 6H, two CH*Me*), 0.47 (d, J = 6.8 Hz, 3H, CH*Me*). ^{19}F NMR: δ −62.6 (s, BAF), −145.7 (m, 2F, TFB), −149.9 (br, 4F, BF_4), −157.4 (m, 2F, TFB).

[Rh(TFB){P(C$_6$H$_4$CHMeNMe$_2$)$_2$(C$_6$H$_4$CHMeNHMe$_2$)}](BF$_4$)$_2$·H$_2$O·Me$_2$CO (8): X-ray Structure. Crystal data and other details of the structure analysis are presented in Table 3. Orange crystals of **8** were obtained through recrystallization by slow diffusion in acetone/hexane.

A crystal of **8** of dimension of 0.42 × 0.40 × 0.30 mm was mounted on a glass fiber with grease. All diffraction measurements were made at low temperature with a Siemens three-circle SMART area detector diffractometer using graphite-monochromated Mo Kα radiation.[34] All subsequent frames were referenced to a dark frame reading taken at 10 s exposures without X-rays. Unit cell dimensions were determined from reflections taken from 3 sets of 15 frames (at 0.3° steps in ω) each at 10 s exposure. A full hemisphere of reciprocal space was scanned by 0.3° ω steps at ϕ 0°, 90°, and 180° with the area detector center held at 2θ = −29°. The reflections were integrated using the SAINT program.[35] A total of 14885 diffracted intensities were measured in a unique hemisphere of reciprocal space for 2θ < 55°. The data were processed and absorption correction was applied with SADABS.[36] Effective transmission coefficients were in the range 1.000 and 0.913, respectively. A total of 10910 unique observations remained after averaging of duplicate and equivalent measurements (R_{int} 0.044) and deletion of the systematic absences. Of these, 9090 had $I > 2\sigma(I)$. Lorentz and polarization corrections were applied.

Table 3. Crystallographic Data for **8**

empirical formula	$C_{45}H_{57}B_2F_{12}N_3O_2PRh$
fw	1055.44
temp	173(2) K
wavelength	0.71073 Å
cryst syst, space group	monoclinic, $P2_1$
unit cell dimens	a = 12.548(11) Å
	b = 16.139(2) Å
	c = 12.1804(10) Å
	β = 100.742(9)°
vol	2328.2(4) Å^3
Z	4
density (calcd)	1.506 Mg/m^3
abs coeff	0.490 mm^{-1}
cryst size	0.42 × 0.40 × 0.30 mm
θ range for data collection	1.72−27.49
reflns collected	14885
indep reflns	10196 [R(int) = 0.0202]
abs correction	SADABS
refinement meth	full-matrix least-squares on F^2
data/restraints/params	10196/1/619
GOF on F^2	1.001
final R indices [$I > 2\sigma(I)$]	R1 = 0.031, wR2 = 0.0668
R indices (all data)	R1 = 0.0373, wR2 = 0.0688
absolute structure param	0.00(2)

(34) SMART Siemens Molecular Analysis Research Tool, V4.014; Siemens Analytical X-ray Instruments, Madison, WI.
(35) SAINT (Siemens Area detector INTegration) program, Siemens Analytical X-ray, Madison, WI.
(36) SADABS (Siemens Area Detector Absorption), G. Sheldrick. University of Göttingen, Germany.

The structure was solved by direct methods and refined using full-matrix least-squares refinement on F^2 with the SHELXTL program[37] on a Silicon Graphics IRIS computer. All non-hydrogen atoms were assigned anisotropic displacement parameters and refined without positional constraints.

All hydrogen atoms were constrained to idealized geometries and assigned isotropic displacement 1.2 times the U_{iso} for methylene and aromatic carbons. Refinement of the 619 least-squares variables converged to residual indices: $R1 = 0.0310$, wR2 = 0.0668, $S = 1.001$. Weights, w, were set equal to $1/[\sigma_c^2(F_o^2) + (aP)^2 + b]^{-1}$ where $P = [\mathrm{Max}(F_o^2,0) + 2F_c^2]/3$, $\sigma_c^2(F_o^2)$ is the variance in F_o^2 due to counting statistics, and $a = 0.0302$, $b = 0.000$ were varied to minimize the variation in S as a function of $|F_o|$. Final difference electron density maps showed no features outside the range +0.976 to −0.550 Å^{-3}, the largest being within 1.08 Å of F(5A). Tables reporting the atomic positional parameters for the freely refined atoms, the derived bond lengths and interbond angles, and the atomic displacement parameters, hydrogen atom parameters, and observed and calculated structure amplitudes are given in Supporting Information.

[Rh(TFB)(PN_3)]BF_4 (9). This compound was prepared as described for **1**, but using PN_3 (296 mg, 0.68 mmol) instead of PN. Yield: 412 mg (71%). Anal. Calcd for $C_{39}H_{42}BF_8N_3PRh$: C, 55.14; H, 4.98; N, 4.95. Found: C, 54.94; H, 5.10; N, 4.53. $^{31}P\{^1H\}$ NMR ($CDCl_3$, 213 K): δ 26.3 (d, $J_{Rh-P} = 172$ Hz). ^1H NMR ($CDCl_3$, 213K): δ 10.25 (dd, 1H, $J = 17.6$ Hz, $J = 7.3$ Hz, Ar), δ 7.93 (m, 2H, Ar), δ 7.79 (m, 1H, Ar), δ 7.70 (m, 1H, Ar), δ 7.55 (m, 2H, Ar), δ 7.45 (m, 1H, Ar), δ 7.35 (m, 2H, Ar), δ 7.17 (m, 1H, Ar), δ 6.97 (m, 1H, Ar), δ 6.03 (m, 1H, *H*-Cbridge(TFB)), δ 5.88 (m, 1H, *Holef-cisN*(TFB)), δ 5.45 (m, 1H, *H*-Cbridge(TFB)), δ 5.33 (m, 1H, *Holef-cisN* (TFB)), δ 4.01 (d, $J = 12.8$ Hz, 1H, CH_2), δ 3.82 (d, $J = 16.5$ Hz, 1H, CH_2), δ 3.38 (d, $J = 16.3$ Hz, 2H, CH_2), δ 3.21 (m, 1H, *Holef-transN* (TFB)), δ 3.16 (d, $J = 15.6$ Hz, 1H, CH_2), δ 2.89 (d, $J = 14.8$ Hz, 1H, CH_2), δ 2.79 (s, 3H, NcoordCH_3), δ 2.43 (s, 6H, N(CH_3)$_2$), δ 2.39 (s, 3H, NcoordCH_3), δ 2.15 (m, 1H, *Holef-transN*(TFB)), δ 1.84 (s, 6H, N(CH_3)$_2$). ^{19}F NMR ($CDCl_3$, 213K): δ −145.60 (m, 1F), −146.71 (m, 1F), −152.02 (s, $^{10}BF_4$), −152.07 (s, $^{11}BF_4$), −158.70 (m, 2F).

[Rh(COD)(PN_3)](BF_4) (10). This compound was prepared as described for **4**, but using PN_3 (435 mg, 1 mmol) instead of PN. Yield: 576 mg (78%). Anal. Calcd $C_{35}H_{48}BF_4N_3PRh$: C, 57.47; H, 6.61; N, 5.75. Found: C, 57.19; H, 6.31; N, 5.88. $^{31}P\{^1H\}$ NMR ($CDCl_3$, 25 °C): δ 21.41 (d, $J_{Rh-P} = 153.3$ Hz). ^1H NMR ($CDCl_3$, 25 °C): δ 10.08 (dd, $J = 16.9$ Hz, $J = 7.4$ Hz, 1H, Ar), δ 8.06 (m, 1H, Ar), δ 7.93 (m, 1H, Ar), δ 7.85 (m, 3H, Ar), δ 7.63 (m, 2H, Ar), δ 7.50 (m, 1H, Ar), δ 7.4−7.2 (m, 3H, Ar), δ 5.60 (m, 1H, C*H*(COD)), δ 5.25 (m, 1H, C*H*(COD)), δ 4.08 (d, $J = 12.8$ Hz, 1H, CH_2), δ 3.81 (d, $J = 15.5$ Hz, 1H, CH_2), δ 3.45 (m, 1H, CH_2), δ 3.39 (a, 2H, CH_2 + C*H*(COD)), δ 3.12 (d, $J = 15.4$ Hz, 1H, CH_2), δ 2.88 (m, 1H, C*H*(COD)), δ 2.80 (s, 3H, NcoordCH_3), δ 2.72 (m, 2H, CH_2 + CH_2(COD)), δ 2.50 (m, 2H, CH_2(COD)), 2.43 (s, 3H, NcoordCH_3), 2.31 (s, 8H, N(CH_3)$_2$ + CH_2(COD)), 1.82 (s, 6H, N(CH_3)$_2$), 1.78 (m, 2H, CH_2(COD)), 1.57 (m, 1H, CH_2(COD)).

Acknowledgment. The Junta de Castilla y León (Project VA120-01) and the Ministerio de Ciencia y Tecnología (Project BQU2001-2015) are very gratefully acknowledged for financial support.

Supporting Information Available: Tables of crystallographic data for the structure **8**, as well as data in CIF format. This material is available free of charge via the Internet at http://pubs.acs.org.

IC034117A

(37) SHELXTL Rev. 5.03, Siemens Analytical X-ray, 1995.